

Original Article

# The natural product Aristolactam AIIIa as a new ligand targeting the polo-box domain of polo-like kinase 1 potently inhibits cancer cell proliferation

Li LI<sup>1, #</sup>, Xu WANG<sup>2, #</sup>, Jing CHEN<sup>2, \*</sup>, Hong DING<sup>2</sup>, Yu ZHANG<sup>2</sup>, Tian-cen HU<sup>2</sup>, Li-hong HU<sup>2, \*</sup>, Hua-liang JIANG<sup>1, 2</sup>, Xu SHEN<sup>1, 2</sup>

<sup>1</sup>School of Pharmacy, East China University of Science and Technology, Shanghai 200237, China; <sup>2</sup>Drug Discovery and Design Center, State Key Laboratory of Drug Research, Shanghai Institute of Materia Medica, Chinese Academy of Sciences, Shanghai 201203, China

**Aim:** To search for novel inhibitors of human polo-like kinase 1 (Plk1), which plays important roles in various aspects of mitotic progression and is believed as a promising anti-cancer drug target, and further investigate the potential inhibition mechanism of active compounds against Plk1, thus developing potent anti-tumor lead compounds.

**Methods:** Surface plasmon resonance (SPR) technology-based assay and enzymatic inhibition assay were used to screen Plk1 inhibitors. Sulphorhodamine B (SRB)-based assay, flow cytometry, confocal microscopy and Western blotting were used to further identify the potent Plk1 inhibitor. To investigate the inhibitory mechanism of the active compound against Plk1, enzymatic inhibition assay, SPR and yeast two-hybrid technology-based assays were used.

**Results:** Aristolactam AIIIa was identified as a new type of Plk1 inhibitors, targeting the Polo Box domain (PBD) which is another efficient tactic for exploring Plk1 inhibitors. Further studies indicated that it could block the proliferations of HeLa, A549, HGC and the HCT-8/V cells (clinical Navelbine-resistant cancer cell), induce mitotic arrest of HeLa cells at G<sub>2</sub>/M phase with spindle abnormalities and promote apoptosis in HeLa cells. The results from SPR and yeast two-hybrid technology-based assays suggested that it could target both the catalytic domain of Plk1 (CD) and PBD and enhance the CD/PBD interaction.

**Conclusion:** Our current work is expected to shed light on the potential anti-tumor mechanism of Aristolactam AIIIa, and this natural product might be possibly used as a lead compound for further developing anti-tumor drugs.

**Keywords:** antitumor drugs; Aristolactam AIIIa; Polo-box domain; Polo-like kinase 1 inhibitor

Acta Pharmacologica Sinica (2009) 30: 1443–1453; doi: 10.1038/aps.2009.141

## Introduction

Polo-like kinases (Plks) belong to a family of Ser/Thr protein kinases and play a variety of roles in cell cycle progression<sup>[1]</sup>. To date, four members of this family have been identified in mammalian cells, termed as Plk1, Plk2 (SNK), Plk3 (PRK/FNK), and Plk4 (SAK)<sup>[2–6]</sup>, of which Plk1 is the best characterized. It has been discovered that Plk1 functions importantly in numerous aspects of mitotic progression, including controlling entry into mitosis through the activation of the cdc2/cyclinB complex<sup>[7]</sup>, centrosome maturation<sup>[8]</sup>, bipolar spindle formation<sup>[8]</sup>, sister chromatid separation<sup>[9]</sup>, anaphase promot-

ing complex activation<sup>[10]</sup> and affecting cytokinesis by phosphorylating NudC<sup>[11]</sup>, etc. Overexpression of Plk1 has been observed in many human tumors including non-small cell lung cancer, oropharyngeal carcinoma, esophageal carcinoma, gastric carcinoma, melanoma, breast cancer, ovarian cancer, endometrial cancer, colorectal cancer, glioblastoma, papillary carcinoma, pancreatic, prostate, hepatoblastoma, and non-Hodgkin's lymphoma<sup>[12]</sup>. In addition, Plk1 expression is also considered to be of prognostic value for patients suffering from varied types of tumors. Furthermore, microinjection of Plk mRNA was proved to be sufficient to drive quiescent cells into mitosis, and constitutive expression of Plk in NIH 3T3 cells could cause oncogenic focus formation<sup>[13]</sup>. Meanwhile, phosphorothioate antisense oligonucleotides (ASOs) against Plk1 showed potent anti-proliferative effect in cell culture and in mouse xenograft studies<sup>[14, 15]</sup>. Therefore, all these above-mentioned results have made Plk1 a potent target for the dis-

# These authors contributed equally to this article.

\* To whom correspondence should be addressed.

E-mail jingchen@mail.shcnc.ac.cn (Jing CHEN)

simmhulh@mail.shcnc.ac.cn (Li-hong HU)

Received 2009-07-09 Accepted 2009-08-19

covery of anti-tumor agents.

Structurally, Plks are homologous and contain two conserved domains, the N-terminal catalytic kinase domain (CD) and the C-terminal polo box domain (PBD) that is composed of so-called polo boxes. The PBD exhibits a critical role in the regulation of Plk1's kinase activity and the subcellular localization of Plk1<sup>[16]</sup>. It has been reported that Plk1 interacts, through its PBD, with certain serine/threonine-phosphorylated proteins localized at particular mitotic apparatuses, and binding of the PBD to the primed phosphorylation sites not only serves for targeting the kinase domain to substrates but also simultaneously activates the kinase domain by relieving the inhibitory intramolecular interaction<sup>[17]</sup>. Therefore, in addition to blocking the ATP-binding or the substrate-binding site, targeting the PBD is also considered as another efficient tactic for the exploration of Plk1 inhibitors.

The first published small molecular Plk1 inhibitor was scytonemin, a natural marine product isolated from cyanobacteria<sup>[18, 19]</sup>, which is a micromolar non-specific ATP competitor. The pharmacophore ON01910 was a non-ATP competitive inhibitor of Plk1, which was probably a substrate-competitive inhibitor of recombinant casein and CDC25C<sup>[20]</sup>. The first small molecule inhibitor targeting the PBD was reported recently<sup>[21]</sup>, which could interfere with Plk1 intracellular localization by inhibiting the function of the PBD.

In the current work, by random screening against our in-house natural product library, we discovered that the natural product Aristolactam AIIIa (Figure 1A), an Aristolactam derivative<sup>[22]</sup>, functions as a new type of ligand targeting the PBD. It could inhibit the proliferation of cancer cells and induce apoptosis and the mitotic arrest at G<sub>2</sub>/M phase with spindle abnormalities. Different from the published Plk1 inhibitors, this natural product not only targeted both the CD and PBD domains, but also enhanced the CD/PBD interaction. Our findings might help to shed light on the possible mechanism of the Aristolactams inhibition against cancer cell proliferation<sup>[23, 24]</sup>, and Aristolactam AIIIa might be used as a potential lead compound for further research.

## Materials and methods

### Plasmid construction

The PBD (residues 326–603 of Plk1) and the catalytic domain of Plk1 (CD, residues 1–370 of Plk1) were amplified by PCR from pUC18-Plk1 (synthesized by Shanghai Sangon Biological Engineering Technology & Services Co, Ltd, Shanghai, China), and then subcloned into the vector pGEX4T-1 and pFastBacHTb, respectively. For the yeast two-hybrid assay, the DNA fragment encoding the PBD was digested with *Eco*R I and *Xho* I (NEB) from the pGEX4T-1-PBD plasmid and then cloned into the pGADT7 vector. Similarly, the catalytic domain of Plk1 was cloned into the pGBKT7 vector from pFsatBacHTA-CD. For overexpression, the PBD and CD were amplified by PCR from pUC18-Plk1 and then subcloned into the vector pCDNA3.1a, respectively.

### Protein preparation

By using pGEX4T-1-PBD as the expression plasmid, the recombinant protein GST-tagged PBD was expressed in *E coli* BL21 (DE3) cells and purified by glutathione-affinity chromatography. The GST tag was cleaved on column with thrombin (Pharmacia) and the native PBD was obtained by gel filtration. The His-tagged catalytic domain of Plk1 was expressed in TN insect cells (TN-5B1-4, Trichoplusia Ni) using standard baculovirus expression protocols and purified with Ni-NTA affinity chromatography.

### *In vitro* enzymatic assays of the full-length Plk1 and its catalytic domain

The enzymatic assays of Plk1 and its catalytic domain were performed using the Cyclex Plk1 assay kit/inhibitor screening kit (Cyclex Co, Japan). Kinase inhibition experiments were carried out according to the protocol provided by the manufacturer. Plates were pre-coated with the substrate termed recombinant Protein-X, which contains a threonine residue that can be phosphorylated by Plk1. The detector antibody specifically detects the phosphorylated threonine on Protein-X. During the assay, Plk1 or its catalytic domain was dissolved in 10  $\mu$ L kinase buffer and mixed with 10  $\mu$ L of compound solution at different concentrations (prepared by diluting 1  $\mu$ L of DMSO mother liquor into 9  $\mu$ L kinase buffer). The mixture was finally added to 80  $\mu$ L of kinase buffer containing 50  $\mu$ mol/L ATP. After pre-incubation at 4 °C for 80 min, the plates were incubated at 30 °C for 30 min, and the wells were washed five times with 1 $\times$ wash buffer provided by the manufacturer. Subsequently, 100  $\mu$ L of anti-phospho-threonine polyclonal antibody (PPT-07) was added to each well and incubated at room temperature for 30 min. The wells were washed five times as described above and incubated with 100  $\mu$ L of HRP-conjugated anti-rabbit IgG. Following a 30-min incubation at room temperature, the wells were washed five times and incubated with 100  $\mu$ L of a chromogenic substrate reagent for 5 min. The reaction was terminated with 100  $\mu$ L stop solution, and the amount of phosphorylated substrate was determined by measuring the absorbance at dual wavelengths of 450/540 nm.

### Immunoprecipitation

For Plk1 immunoprecipitation, HeLa cells (4 $\times$ 10<sup>6</sup> cells/well) were seeded on 10-mm dish and incubated overnight. After incubation with nocodazole (5  $\mu$ g/mL) for 12 h, the cells were lysed with 500  $\mu$ L cold lysis buffer containing a protease inhibitor cocktail. The cell lysate was treated with 500  $\mu$ L of lysis buffer containing 10  $\mu$ L of a prepared protein A/G bead slurry 1 h at 4 °C and then centrifuged at 13 000 r/min for 15 min at 4 °C. The supernatant was carefully collected without disturbing the pellet and transferred to a clean tube, followed by incubation with 10  $\mu$ L of Plk1 antibody (1:50, 35–306 aa, Abcam) overnight. After incubated with 20  $\mu$ L pre-cleared protein A/G bead slurry at 4 °C for 3 h on a rotator, the mixture was spun at 13 000 r/min for 2 min at 4 °C. The supernatant was

carefully removed and the beads were washed twice with 50  $\mu$ L kinase buffer. After the final wash, the agarose beads were resuspended in 50  $\mu$ L kinase buffer and mixed gently. The catalytic domain of Plk1 (residues 1–370 of Plk1) that was transiently transfected into 293T cells for 48 h was immunoprecipitated with an anti-myc antibody (1:400, Invitrogen).

#### Sulphorhodamine B-based assay for cell proliferation

The quantitative sulphorhodamine B (SRB) colorimetric assay<sup>[25]</sup> was used for determining the inhibition of Aristolactam AIIIa against HGC, A549, HeLa, and HCT-8/V cancer cells. Cells were seeded onto a 96-well plate with 5000 cells per well and incubated at 37 °C for 24 h. The cells were treated with increasing concentrations of Aristolactam AIIIa for another 72 h, fixed with 10% trichloroacetic acid for 1 h at 4 °C, air-dried, and then stained at room temperature for 20 min with 4 mg/mL SRB solution. Cells were subsequently washed with 1% acetic acid five times and dissolved in 150  $\mu$ L of 10 mmol/L Tris buffer. The cell viability was presented as absorbance at 515 nm (Benchmark Plus™ microplate spectrophotometer, BIO-RAD) and averaged from three replicates. The values were obtained from three independent experiments. NVB (Navelbine) and DMSO were used as positive and negative controls, respectively. All cell culture reagents were purchased from Gibco.

#### Analysis of cell cycle progression

HeLa cells ( $3 \times 10^4$  cells/well) were seeded onto 6-well plates and incubated overnight. After being incubated with Aristolactam AIIIa (10  $\mu$ mol/L) for 24 or 48 h, the adherent cells were detached with trypsin, and the floating cells were collected by centrifugation at  $600 \times g$  for 10 min. The cells were washed twice with PBS, fixed in 75% ethanol-PBS at 4 °C for 2 h, and then collected by centrifugation. Cells were resuspended with 500  $\mu$ L PBS containing 100 mg/mL RNase A and incubated for 30 min at 37 °C, followed by filtration and staining with 0.5 mg/mL propidium iodide (PI) for 1 h. The suspensions were then analyzed by Becton Dickinson FACScan (BD Biosciences, San Jose, CA). The percentage of cells in the G<sub>0</sub>/G<sub>1</sub>, G<sub>2</sub>/M phases of the cell cycle was determined by the DNA contents.

#### Confocal microscopy

HeLa cells grown on glass coverslips were washed with PBS and fixed in 4% paraformaldehyde. After washed with PBS for 5 min, the fixed cells were treated with PBS containing 1% Triton at room temperature for 10 min and then washed with PBS containing 0.02% Tween 20 for 5 min. To image the spindle apparatus, the fixed cells were incubated with a FITC-conjugated monoclonal anti- $\alpha$ -tubulin antibody (DM1A, Sigma) at a 1:100 dilution and propidium iodide (PI) at 37 °C for 45 min. In Plk1 localization assay, the antibodies used were the mouse monoclonal antibody (mAb) anti-Plk1 (1:200; 35–306 aa; Abcam) and the Alexa Fluor 488-conjugated goat anti-mouse (1:1000; Invitrogen) antibody. DNA was stained

with PI. Coverslips were washed with PBS, 50% glycerol was applied on the slide, and the coverslip was added on top with the cells facing the glycerol and sealed with glycerol. The stained cells were imaged by the confocal microscope (Leica, German) with a 63 $\times$  objective.

#### Apoptosis assay

HeLa cells ( $3 \times 10^4$  cells/well) were seeded onto 24-well plates and, after overnight incubation, the cells were incubated with Aristolactam AIIIa (10  $\mu$ mol/L) for 24 h. The PARP cleavage assay was performed with equal amounts of total cellular proteins that were resolved on a 10%-SDS-polyacrylamide gel, and Western blotting analysis was performed using anti-PARP antibodies (BD Biosciences).

In Annexin V apoptosis assay, HeLa cells were seeded onto six-well plates and after overnight incubation, cells were incubated with Aristolactam AIIIa (10  $\mu$ mol/L) for 24 h. Cells were trypsinized and incubated with Annexin V according to the manufacturer's recommendations (Calbiochem).

#### Surface plasmon resonance (SPR) technology-based binding assay

The binding of Aristolactam AIIIa to the PBD or CD was analyzed by SPR technology-based Biacore 3000 instrument (Biacore AB, Uppsala, Sweden). All experiments were carried out using HBS-EP (10 mmol/L HEPES pH 7.4, 150 mmol/L NaCl, 3.4 mmol/L EDTA and 0.005% surfactant P20) as running buffer with a constant flow rate of 30  $\mu$ L/min at 25 °C. The PBD protein, which was diluted in 10 mmol/L sodium acetate buffer (pH 4.2) to a final concentration of 2  $\mu$ mol/L, was covalently immobilized on the hydrophilic carboxymethylated dextran matrix of the CM5 sensor chip (BIAcore) using standard primary amine coupling procedure. The CD protein, which was diluted in 10 mmol/L sodium acetate buffer (pH 4.13) to a final concentration of 2  $\mu$ mol/L, was immobilized on the chip using the same procedure. Aristolactam AIIIa was dissolved in the running buffer at different concentrations ranging from 1 to 10  $\mu$ mol/L. All data were analyzed by BIAevaluation software, and the sensorgrams were processed by automatic correction for nonspecific bulk refractive index effects. The kinetic analyses of the Aristolactam AIIIa/PBD binding were performed based on the steady state affinity fit model according to the procedures described in the software manual, and the Aristolactam AIIIa/CD binding equilibrium dissociation constant was calculated based on the 1:1 Langmuir binding fit model.

To investigate the effect of Aristolactam AIIIa on the PBD/CD interaction, the purified CD protein was immobilized on a CM5 sensor chip. After the PBD (14  $\mu$ mol/L) was incubated with different concentrations of Aristolactam AIIIa (0, 24, 34.3, 49, 70, and 100  $\mu$ mol/L) for 1 h, the samples were applied to the sensor chip at a flow rate of 10  $\mu$ L/min for 60 s, followed by washing with HBS-EP 180 s. The binding ability of PBD towards the CD was reflected by RU values recorded directly by the Biacore 3000 instrument.

### Yeast two-hybrid assay

Competent cells of the yeast strain AH109 were obtained from Clontech (Plano Alto, CA), and transformations were performed according to the manufacturer's protocol. First, 500 ng of plasmid DNA was added to 50  $\mu$ L of competent cells and mixed with 36  $\mu$ L of 1 mol/L lithium acetate, 5  $\mu$ L of boiled 10 mg/mL ss-carrier DNA and 240  $\mu$ L of 50% poly(ethylene glycol) (MW3350) at 30  $^{\circ}$ C for 30 min followed by heat-shock at 42  $^{\circ}$ C for 30 min and subsequently spread on a drop-out-agar plate that lacked leucine and tryptophan. The plates were incubated at 30  $^{\circ}$ C for 48 h to allow for yeast growth. PCR was used to confirm the transformation of the target plasmids. A positive clone was inoculated into SD medium lacking leucine and tryptophan (SD-LT) overnight, the culture was then diluted to OD<sub>600</sub> of 0.003 with SD medium lacking leucine, tryptophan, and histidine (SD-LTH) which was supplemented with 2 mmol/L of 3-amino-10,20,40-triazole (SD-LTH+3-AT) and 100  $\mu$ mol/L of Aristolactam AIIIa. The medium was shaken at 250 r/min at 30  $^{\circ}$ C for 48 h before 200  $\mu$ L of the culture was added to the well of a 96-well microplate. The absorbance at 600 nm of the culture in the 96-well microplate was then measured by a Benchmark Plus<sup>TM</sup> microplate spectrophotometer (BIO-RAD). This is an alternative method based on the growth curve analysis for yeast culture that is amenable to a microtiter plate format. It is reproducible and of equal or

greater sensitivity compared with the  $\beta$ -galactosidase assay<sup>[26]</sup>. All the yeast media were prepared according to the standard Protocols Handbook (PT3024-1, Clontech).

### Results

#### Aristolactam AIIIa inhibits Plk1 activity

To evaluate the inhibition of Aristolactam AIIIa against Plk1, the Polo-like kinase1 Assay/Inhibitor Screening Kit (Cyclex Co, Japan) was used. During the assay, 1.25 munits of recombinant Plk1 (Cyclex Co, Japan) was mixed with different concentrations of either Aristolactam AIIIa or DMSO (as a control), and the kinase activity was measured by using Protein-X as substrate. As indicated in Figure 1B, the natural product Aristolactam AIIIa exhibited a dose-dependent inhibition against Plk1-mediated phosphorylation of Protein-X with an IC<sub>50</sub> value of 47.5  $\mu$ mol/L.

In order to further confirm the inhibition of Aristolactam AIIIa against Plk1, the kinase activity of endogenous Plk1 immunoprecipitated from Nocodazole-arrested HeLa cells was measured after incubation with Aristolactam AIIIa (10  $\mu$ mol/L and 100  $\mu$ mol/L) or DMSO (as a control). As shown in Figure 1C, Aristolactam AIIIa also inhibited the endogenous Plk1 activity in a dose-dependent manner.

To investigate the potential selectivity of Aristolactam AIIIa against Plks, the inhibition of Aristolactam AIIIa against

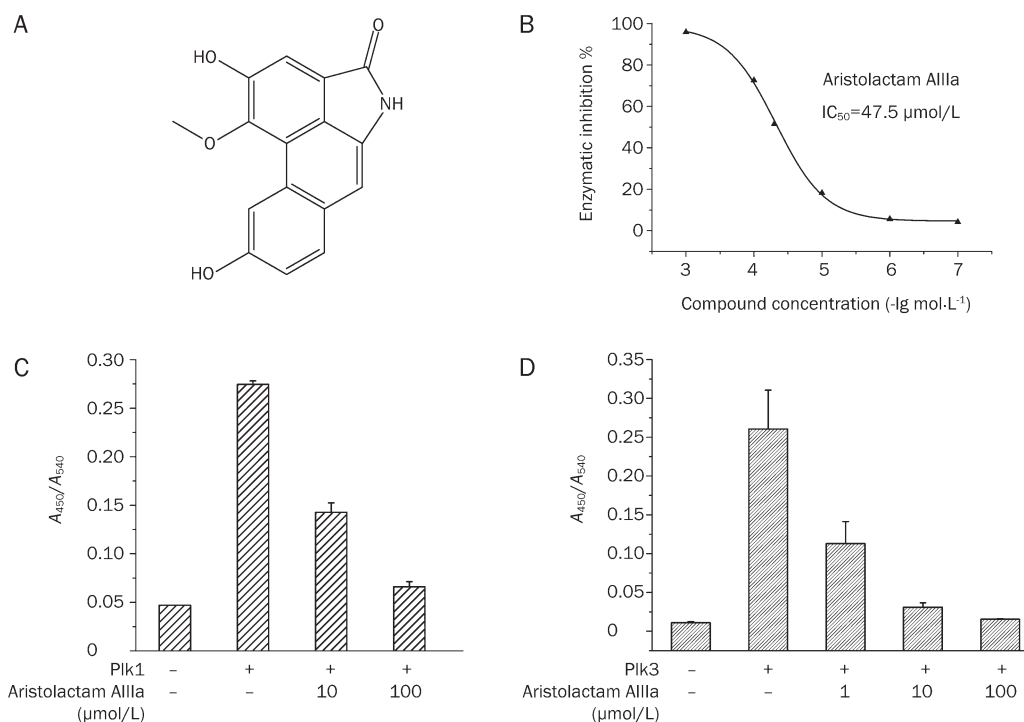


**Figure 1.** Aristolactam AIIIa could inhibit the Plk1 catalytic activity. (A) Structure of Aristolactam AIIIa. (B) Inhibition of Aristolactam AIIIa against Plk1 catalytic activity. Plk1 ( $1.25 \times 10^{-3}$  units) was pre-incubated with Aristolactam AIIIa at different concentrations, and the inhibited Plk1 activity was presented as percentage of the maximal inhibition.  $\blacktriangle$ , Aristolactam AIIIa (0.1, 1, 5, 10, 50, 100, and 1000  $\mu\text{mol/L}$ ). All data were averaged from three independent experiments. Half-maximal inhibitor concentrations (IC<sub>50</sub> values) were obtained by sigmoidal fit of inhibitory curves using Origin 7.0. (C) Inhibition of Aristolactam AIIIa against the endogenous Plk1 enzyme immunoprecipitated from mitotic cells (Nocodazole-arrested HeLa cells). Plk1 was pre-incubated with Aristolactam AIIIa (10 and 100  $\mu\text{mol/L}$ ) or DMSO for 1 h. (D) Inhibition of Aristolactam AIIIa against Plk3 catalytic activity. Plk3 was pre-incubated with Aristolactam AIIIa (1, 10, and 100  $\mu\text{mol/L}$ ) or DMSO for 1 h.

Plk3 was measured with a Polo-like kinase3 Assay/Inhibitor Screening Kit (Cyclex Co, Japan). As shown in Figure 1D, Aristolactam AIIIa exhibited a dose-dependent inhibition against Plk3, indicating that Aristolactam AIIIa had no selectivity for Plks.

#### Aristolactam AIIIa inhibits the proliferation of human HeLa, A549, HGC, and HCT-8/V cells

As has been reported<sup>[24]</sup>, some Aristolactam derivatives could exhibit cytotoxicity against KB, P388, A549, HT29, HL60, HeLa, and L1210 cells, but no detailed inhibition mechanism was investigated. Although Aristolactam AIIIa has been reported to inhibit platelet aggregation induced by collagen and AA, its anti-tumor activity has not yet been elucidated<sup>[27]</sup>. Here, the anti-proliferation effect of Aristolactam AIIIa on HeLa, A549, and HGC cancer cell lines was examined. As shown in Table 1 and Figure 2A, Aristolactam AIIIa inhibited the proliferation of these cancer cells in a dose-dependent manner with  $IC_{50}$  values ranging from 7 to 30  $\mu\text{mol/L}$ . Moreover, to further explore the potential inhibition of Aristolactam AIIIa against the relevant clinical drug-resistant cancer cell, the Navelbine (NVB)-resistant HCT-8/V cell line was assayed. As indicated in Figure 2B and Table 2, Aristolactam AIIIa exhibited dose-dependent inhibitory effects on HCT-8/V with an  $IC_{50}$  of 3.55  $\mu\text{mol/L}$ , even while 10  $\mu\text{mol/L}$  of NVB had no effect on HCT-8/V proliferation.

**Table 1.** Anti-proliferation activity of Aristolactam AIIIa against different cancer cell lines.

Cancer cell line	HeLa	A549	HGC
$IC_{50}$ ( $\mu\text{mol/L}$ )	7.98	15	31

**Table 2.** Susceptible property of clinical drug-resistant cell line HCT-8/V to Aristolactam AIIIa.

	$IC_{50}$ ( $\mu\text{mol/L}$ )
Aristolactam AIIIa	3.55
NVB	NI

NI: no inhibition at 10  $\mu\text{mol/L}$ .

#### Aristolactam AIIIa induces cell cycle arrest in the $G_2/M$ phase with spindle abnormalities in HeLa cells

Plk1 was shown to be essential to mitotic progression and cytokinesis, and functional down-regulation of Plk1 (either by microinjecting Plk1-specific antibodies or overexpressing dominant-negative Plk1) might induce  $G_2/M$  arrest<sup>[8, 28]</sup>. With these facts in mind, we thereby investigated the potential effect of Aristolactam AIIIa on the cell cycle of tumor cells. As shown in Figure 2C, incubation of HeLa cells with 10  $\mu\text{mol/L}$  of Aristolactam AIIIa for 24 h increased the cell population staying in

$G_2/M$  phase by 100% compared with the control cells, which thus suggested that Aristolactam AIIIa was able to induce cell cycle arrest at the  $G_2/M$  phase. To further confirm this result, the cell cycle distribution pattern of HeLa cells treated for 48 h with Aristolactam AIIIa or DMSO was also investigated. As shown in Figure S1, similar to the case in 24 h incubation, a 48 h incubation with Aristolactam AIIIa could also induce cell cycle arrest in  $G_2/M$  phase.

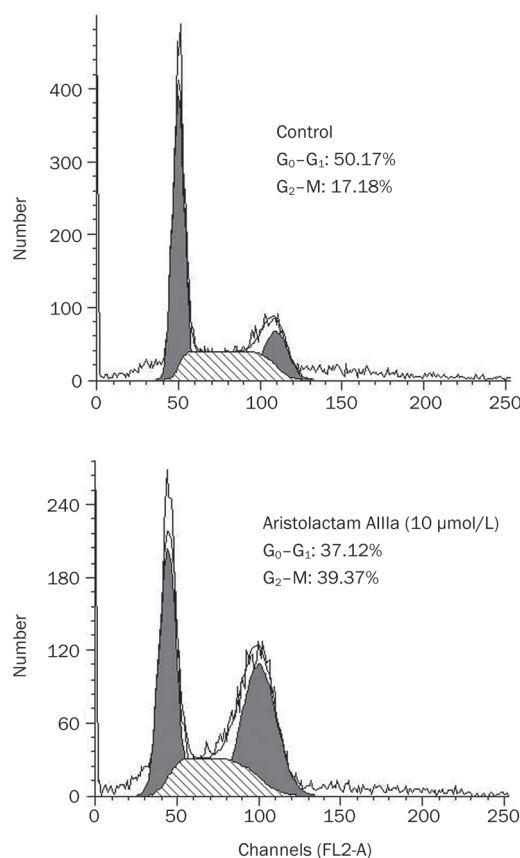


**Figure S1.** Aristolactam AIIIa could induce mitotic arrest of HeLa cells at  $G_2/M$ . Flow Cytometry result showed that the  $G_2/M$  population of HeLa cells increased by 100% after 48 h incubation with the natural product Aristolactam AIIIa (10  $\mu\text{mol/L}$ ).

It has been known that Plk1 is involved in bipolar spindle formation which requires proper spindle assembly. Cells injected with anti-Plk1 antibodies display striking defects in their ability to assemble bipolar spindles, as manifested by the lack of focused spindle poles and unstable attachment of the chromosomes to the spindles<sup>[8, 29]</sup>. To test whether Aristolactam AIIIa could affect spindle assembly, we used confocal laser microscopy to image the spindle apparatus and chromosomes of Aristolactam AIIIa-treated cells. HeLa cells were incubated with either DMSO (as a control) or 10  $\mu\text{mol/L}$  of Aristolactam AIIIa for 12 h, fixed with 4% paraformaldehyde, and then stained with FITC conjugated anti- $\alpha$ -tubulin antibody (to visualize tubulin spindles) and propidium iodide

(to visualize chromosomal DNA). The images showed that the most DMSO-treated cells at mitosis phase exhibited no abnormality while 70% of the Aristolactam AIIIa-treated cells displayed multipolar spindles and misaligned chromosomes (Figure 2D and 2E). Such results were in agreement with the previous results for Plk1-depleted cells<sup>[29]</sup>, and suggested that Aristolactam AIIIa could induce aberrant spindle assembly in cells through its inhibition against Plk1.

#### Aristolactam AIIIa induces apoptosis of cancer cells

Considering that the activation of apoptotic pathways could

be detected by examining PARP (Poly [ADP-ribose] polymerase-1) cleavage<sup>[30]</sup>, a marker for caspase activation, we thereby examined the potential effects of Aristolactam AIIIa on the apoptosis of HeLa cells by determining the induction of the cleaved PARP p85 fragment. Western blot analysis showed PARP cleavage in Aristolactam AIIIa-treated HeLa cells (Figure 3A), indicating the apoptosis induction in these cells. This result is consistent with the reported effects of Plk1 siRNA<sup>[31]</sup> and other Plk1 inhibitors on cancer cells<sup>[20, 32]</sup>.

To further confirm the above results, Aristolactam AIIIa (10  $\mu\text{mol/L}$ ) or DMSO-treated HeLa cells were labeled with

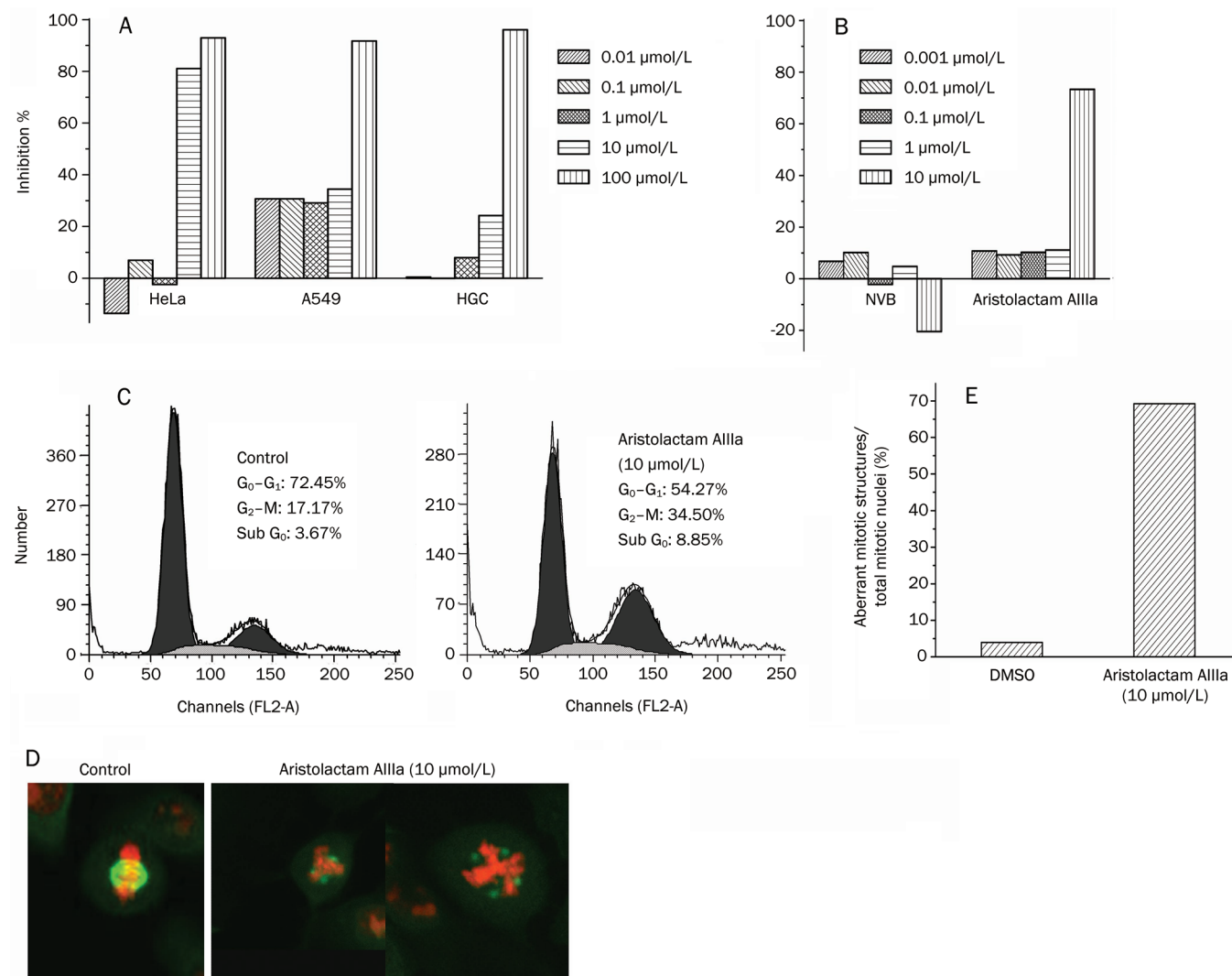


**Figure 2.** Aristolactam AIIIa could inhibit the proliferation of cancer cells and induce mitotic arrest at  $G_2/M$  with spindle abnormalities. (A) Aristolactam AIIIa inhibited the proliferation of cancer cells in a dose-dependent manner. HeLa, A549, and HGC cells were cultured in the presence of increasing concentrations of Aristolactam AIIIa. (B) Aristolactam AIIIa inhibited the proliferation of the clinical drug-resistant cell (HCT-8/V) in a dose-dependent manner. HCT-8/V cells were cultured in the presence of increasing concentrations of Aristolactam AIIIa or NVB. SRB assay was used to determine the cell viability. Each value was averaged from three independent experiments. Half-maximal inhibitory concentrations ( $IC_{50}$  values) were obtained by sigmoidal fit of inhibitory curves using Origin 7.0. (C) Flow Cytometry result showed that the  $G_2/M$  population of HeLa cells increased by 100% after being treated with the natural product Aristolactam AIIIa. (D) Aristolactam AIIIa induced spindle abnormalities in HeLa cells. HeLa cells were treated with either DMSO or 10  $\mu\text{mol/L}$  of Aristolactam AIIIa for 12 h, fixed with 4% paraformaldehyde, and stained with anti- $\alpha$ -tubulin antibody (FITC conjugated) and propidium iodide. The cells were subsequently imaged by confocal laser microscopy. (E) The total percentage of mitotic nuclei with aberrant mitotic structures versus total mitotic nuclei in each treatment group was summarized after 12 h of Aristolactam AIIIa treatment to HeLa cells.

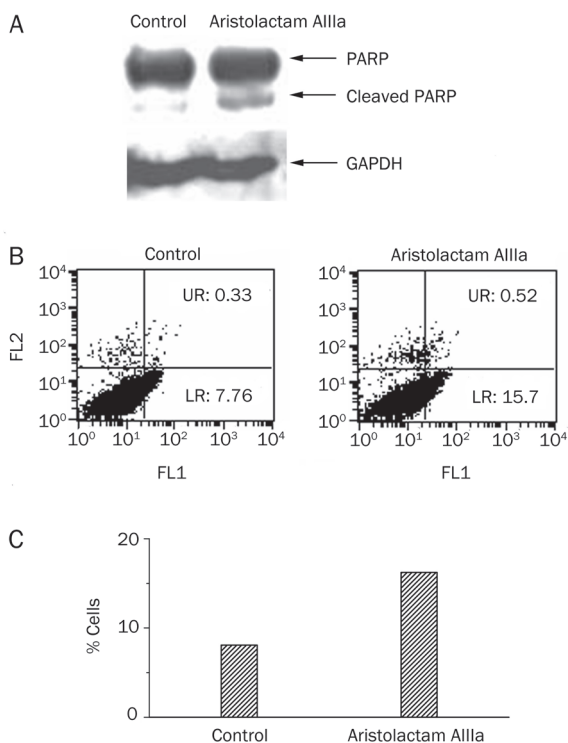


**Figure 3.** Aristolactam AIIIa induces apoptosis in cancer cells. (A) Western blot analysis of cell lysates treated with DMSO or Aristolactam AIIIa (10  $\mu\text{mol/L}$ ) using anti-PARP antibody to assess the cleavage of PARP. (B) HeLa cells treated with DMSO or Aristolactam AIIIa (10  $\mu\text{mol/L}$ ) for 24 h were stained using FITC-conjugated Annexin V and PI and subjected to flow cytometric analysis following the manufacturer's protocol. The lower right (LR) quadrant of the FACS histograms indicates the percentage of early apoptotic cells (Annexin V-positive) and the upper right (UR) quadrant indicates the percentage of late apoptotic cells (Annexin V- and PI-positive). (C) The total percentage of apoptotic cells in each treatment group was summarized after 24 h of Aristolactam AIIIa treatment to HeLa cells.

Annexin V and PI to determine the extent of cellular apoptosis. As shown in Figure 3B and 3C, Aristolactam AIIIa induced an elevated percentage of apoptotic cells including early phase apoptosis (Annexin V-positive) and late phase apoptosis (Annexin V- and PI-positive) compared with DMSO-treated cells.

Moreover, this phenomenon was also confirmed by the analysis of the cell cycle distribution pattern of HeLa cells with 24 h incubation of Aristolactam AIIIa. As shown in Figure 2C, the population of sub- $G_0/G_1$  peaks were 3.67% (DMSO) and 8.85% (Aristolactam AIIIa 10  $\mu\text{mol/L}$ ), respectively, indicating Aristolactam AIIIa could induce apoptosis of cancer cells.

#### Aristolactam AIIIa binds to the catalytic domain of Plk1 and inhibits its activity

In order to further scrutinize the possible inhibition mechanism of Aristolactam AIIIa against Plk1, the binding and inhibition features of Aristolactam AIIIa against the Plk1 PBD and CD domains were characterized.

SPR technology-based Biacore 3000 instrument was used to carry out the kinetic analysis of Aristolactam AIIIa binding to the CD. In the assay, the 1:1 Langmuir binding fit model was used to determine the equilibrium dissociation constant ( $K_D$ ), and the accuracy of the obtained results was evaluated by  $\chi^2$ . As indicated in Figure 4A and Table 3, Aristolactam AIIIa

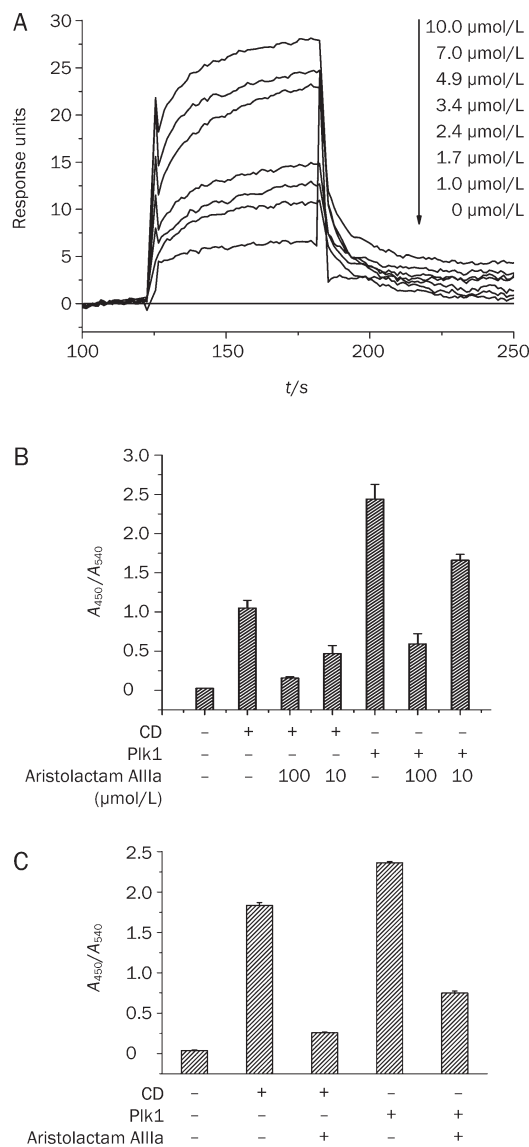


**Figure 4.** Aristolactam AIIIa binds to the catalytic domain (CD) of Plk1 and inhibits its activity. (A) SPR technology based kinetic analysis of CD/Aristolactam AIIIa interaction. Sensorgrams of Aristolactam AIIIa binding to CD measured by SPR technology based Biacore 3000 instrument. Representative sensorgrams were obtained from injecting Aristolactam AIIIa with concentrations of 0, 1, 1.7, 2.4, 3.4, 4.9, 7.0, and 10.0  $\mu\text{mol/L}$  over CD immobilized on the CM5 chip. (B) Inhibition of purified recombinant CD activity by Aristolactam AIIIa. 0.03 mg/mL of CD was mixed with DMSO (as a control) or Aristolactam AIIIa (100  $\mu\text{mol/L}$  and 10  $\mu\text{mol/L}$ ) and the kinase activity was measured. (C) Inhibition of Aristolactam AIIIa against CD immunoprecipitated from transiently transfected 293T cells. The kinase activity was measured by incubation with Aristolactam AIIIa (100  $\mu\text{mol/L}$ ) or DMSO (as a control).

**Table 3.** SPR technology based kinetic analysis for PBD or CD/Aristolactam AIIIa interaction.

Target	$K_D$ ( $\mu\text{mol/L}$ )*	$\chi^2$
CD	1.44	0.353
PBD	2.99	3.28

\* $K_D$ , equilibrium dissociation constant;  $\chi^2$ , statistical value in BIAevaluation; CD, catalytic kinase domain; PBD, polo box domain.

exhibits a high binding affinity against CD with a  $K_D$  of 1.44  $\mu\text{mol/L}$ .

To test the enzymatic inhibition of Aristolactam AIIIa against the CD, we conducted a similar kinase inhibition assay against the purified recombinant CD (residues 1–370 of Plk1). During the assay, after incubation of the CD with DMSO (as a control) or Aristolactam AIIIa (100  $\mu\text{mol/L}$  and 10  $\mu\text{mol/L}$ ), the kinase activity was measured as described above. As indicated in Figure 4B, Aristolactam AIIIa exhibited a dose-dependent inhibition against the CD. To further confirm this inhibition, the kinase activity of the CD immunoprecipitated from the CD transiently transfected 293T cells was also mea-

sured as incubated with Aristolactam AIIIa (100  $\mu\text{mol/L}$ ) or DMSO (as a control). The results listed in Figure 4C have thereby validated the Aristolactam AIIIa inhibition against the CD.

Taken together, the above results have suggested that Aristolactam AIIIa could directly bind the catalytic domain of Plk1 and inhibit its activity.

### Aristolactam AIIIa targets the PBD and increases the PBD/CD interaction

The auto-inhibitory mechanism of Plk1 by its intrinsic Polo box domain (PBD) has made the PBD as another potential target besides the catalytic domain. To investigate whether Aristolactam AIIIa could interfere with PBD function through its binding to the PBD, the binding affinity of Aristolactam AIIIa against PBD was studied by using the SPR technology-based Biacore 3000 instrument. In the assay, immobilization of the PBD on the Biacore biosensor chip resulted in a resonance signal of 7540 resonance units (RUs). The results in Figure 5A indicated the dose-dependent biosensor RUs for Aristolactam AIIIa, suggesting that this natural product could bind to the PBD *in vitro*. The steady state affinity fit model was used to determine the equilibrium dissociation constant  $K_D$ , and the

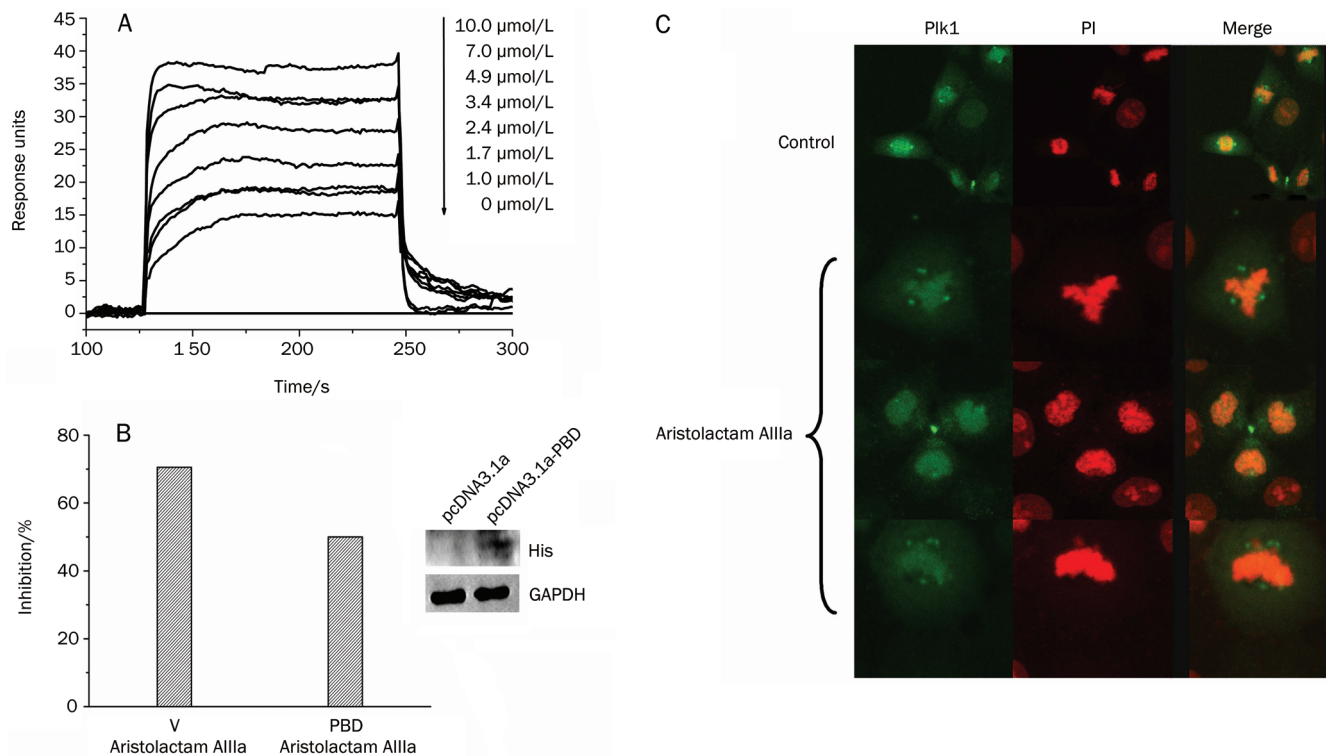


**Figure 5.** Aristolactam AIIIa targets polo box domain (PBD) and does not alter the localization of endogenous Plk1. (A) Sensorgrams of Aristolactam AIIIa binding to PBD measured by SPR technology based Biacore 3000 instrument. Representative sensorgrams were obtained from injecting Aristolactam AIIIa with concentrations of 0, 1.2, 1.7, 2.4, 3.4, 4.9, 7.0, 9.0, and 10.0  $\mu\text{mol/L}$  over PBD immobilized on the CM5 chip. (B) Over expressing PBD could reduce the effect of Aristolactam AIIIa on HeLa cells proliferation. HeLa cells transiently transfected with PBD-pcDNA3.1a or pcDNA3.1a were incubated Aristolactam AIIIa or DMSO respectively. SRB assay was used to determine the cell viability. Inset: the PBD protein level was increased by transfected pcDNA3.1a-PBD in HeLa cells. (C) Aristolactam AIIIa does not alter the localization of endogenous Plk1. HeLa cells were treated with either DMSO or 10  $\mu\text{mol/L}$  of Aristolactam AIIIa for 24 h. Then the cells were analyzed by indirect immunofluorescence microscopy using an anti-Plk1 N-terminal antibody (green), PI (red).



accuracy of the obtained results were evaluated by  $\chi^2$ . The fitted kinetic parameters listed in Table 3 thus demonstrated a strong binding affinity of Aristolactam AIIIa towards the PBD with a  $K_D$  value at 2.99  $\mu\text{mol/L}$ .

In addition, cell-based assay was also carried out to further examine the potential targeting of Aristolactam AIIIa against the PBD in the PBD over-expressing HeLa cells. After transient transfection with pCDNA3.1a-PBD, HeLa cells were incubated with Aristolactam AIIIa at 10  $\mu\text{mol/L}$  for 48 h. As shown in Figure 5B, Aristolactam AIIIa could exhibit inhibitory effects by 50% on the proliferation of the PBD over-expression in HeLa cells in the SRB assay. Compared with the 71% inhibition by Aristolactam AIIIa against the proliferation of the HeLa cells transfected with empty vector (Figure 5B), the result supports the finding that Aristolactam AIIIa targets the PBD.

Since the PBD plays a critical role in Plk subcellular localization<sup>[33]</sup> and Aristolactam AIIIa has been suggested to target the PBD as mentioned above, the localization of endogenous Plk1 in Aristolactam AIIIa or DMSO-treated HeLa cells was thereby examined by using an antibody directed against the N terminus of Plk1 (35–206 aa). As indicated in Figure 5C, in Aristolactam AIIIa-treated cells at mitosis phase, endogenous Plk1 was detected on spindle poles and concentrated close to the midbody in the postmitotic bridges connecting the dividing cells, which is consistent with the founded in DMSO-treated cells.

As has been reported, the PBD is believed to regulate Plk1 activity through its intramolecular interaction with the catalytic domain (CD)<sup>[16, 17]</sup>. Considering this fact, we have thus inspected the potential influence of Aristolactam AIIIa on the PBD/CD interaction by yeast two-hybrid system and SPR technology. In the yeast two-hybrid assay, the yeast cells transformed with both PBD and CD were incubated with either 100  $\mu\text{mol/L}$  Aristolactam AIIIa or DMSO (as a control) for 48 h. The result in Figure 6A implied that Aristolactam AIIIa increased the PBD binding to the catalytic domain of Plk1 by ~43%. Additionally, such Aristolactam AIIIa-stimulated PBD/CD interaction was also confirmed *in vitro* by SPR technology-based assay (Figure 6B).

Summarily, all the above results indicated that Aristolactam AIIIa targets both the PBD and CD. It interferes with the PBD function through the inhibition of Plk kinase activity by increasing the PBD/CD interaction without affecting Plk1 localization to the proper subcellular substructure.

## Discussion

Plk1 plays essential roles in numerous aspects of mitotic progression. A number of studies have demonstrated that Plk1 is over-expressed in a broad spectrum of human tumors<sup>[12]</sup>, and Plk1 has been determined as an attractive target for cancer therapy. To date, three kinds of small molecular inhibitors of Plk1 have been discovered: ATP competitive inhibitor, substrate competitive inhibitor and the PBD inhibitor.

In general, the ATP-binding domain is a regular target for protein kinase inhibitor discovery. However, specificity of

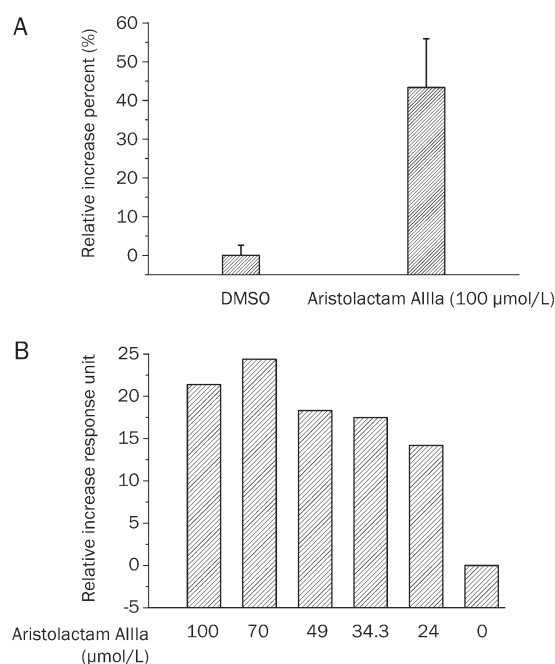


**Figure 6.** Aristolactam AIIIa could increase polo box domain (PBD) binding to the catalytic domain (CD) of Plk1. (A) Aristolactam AIIIa could increase PBD binding to CD as indicated by the yeast two-hybrid technology based assay. The yeast strain AH109 transformed with both PBD and CD was incubated with either 100  $\mu\text{mol/L}$  of Aristolactam AIIIa or DMSO (as a control) for 48 h. The growth curve was tested by measure the absorbance at 600 nm of the culture. (B) Aristolactam AIIIa could increase PBD binding to CD by SPR experiment. The RU values were obtained by injection of PBD (14  $\mu\text{mol/L}$ ) incubated with series of concentrations of Aristolactam AIIIa over the immobilized CD surface.

such target-based inhibitor is difficult to obtain due to the high degree of structural conservation among ATP-binding pockets, and only a few ATP-like inhibitors of Plk1 have so far been published. The first small molecule Plk1 inhibitor was scytonemin, a non-specific ATP competitor, which exhibited comparable potencies against other Ser/Thr and Thr/Tyr kinases including MYT1, CHK1, CDK1, and PKC<sup>[18, 19]</sup>.

Exploration of Plk1 non-ATP competitor is another choice for a Plk1 specific inhibitor in anti-tumor drug discovery. For example, the pharmacophore ON01910 was reported to be a substrate-competitive inhibitor of recombinant casein and CDC25C<sup>[20]</sup>. Another strategy in the development of Plk1 specific inhibitor is to target the PBD, which has a critical role in the regulation of the kinase activity and the subcellular localization of Plk1<sup>[16]</sup>. Recently, the first small molecule targeting the PBD was reported, which could interfere with Plk1 intracellular localization by inhibiting the function of the PBD<sup>[21]</sup>.

Aristolactams are phenanthrene lactam alkaloids that are structurally and biogenetically related to aporphines, which have been reported to show inhibitory activity against cancer cell proliferation; however, the relevant detailed data still remain unclear<sup>[23, 24]</sup>. As a member of Aristolactams, Aristolactam AIIIa demonstrated significant inhibition of platelet

aggregation induced by collagen and AA<sup>[27]</sup>, while its anti-tumor activity has not yet been elucidated. By random screening against the in-house natural product library, we discovered that Aristolactam AIIIa functions as a new type of ligand targeting the PBD, as investigated by the SPR and enzymatic inhibition assays. It could inhibit the proliferation of HeLa, A549, HGC, and HCT-8/V cells, influence cell cycle progression and spindle assembly in HeLa cells and induce the apoptosis in HeLa cells.

Enzymatic characterization indicated that Aristolactam AIIIa could exhibit inhibition activity against the CD, which might contribute to its inhibition against the full length Plk1 *in vitro*, similar to previously published inhibitors<sup>[20,32]</sup>.

To further investigate the potential inhibition mechanism of Aristolactam AIIIa against Plk1, the kinetic feature of Aristolactam AIIIa binding to the PBD was assayed. SPR results demonstrated a strong binding affinity of Aristolactam AIIIa to the PBD ( $K_D=2.99 \mu\text{mol/L}$ ). Since the PBD has a critical role in the regulation Plk1's kinase activity by interacting with the catalytic domain of Plk1<sup>[16,17]</sup>, the result that Aristolactam AIIIa could enhance the PBD interaction with the CD as indicated by SPR and yeast two-hybrid-based assays has shown that this natural product further strengthened the self-regulatory effect of the PBD on Plk1.

It is noticed that the small molecule inhibitors reported by Reindl *et al*<sup>[21]</sup> inhibited the function of the Plk1 PBD and interfered with the intracellular localization of Plk1, while Aristolactam AIIIa did not affect the localization of Plk1. Such discrepancy might possibly come from the different PBD binding sites for the compounds. The reported inhibitors<sup>[21]</sup> interfered with the interaction between PBD and its intracellular anchoring sites of the substrates, resulting in mis-localization of Plk1. However, Aristolactam AIIIa enhanced the CD/PBD interaction, thereby inhibiting Plk1 activity without affecting Plk1 localization. All these findings thus revealed that the regulation of PBD in Plk1's kinase activity and the subcellular localization of Plk1 are closely related to the PBD binding sites.

In summary, we have identified the Aristolactam derivative, Aristolactam AIIIa as a new type of ligand targeting the PBD by random screening our in-house natural product library. Cell-based assays indicated that this natural product could inhibit the proliferation of HeLa, A549, HGC, and HCT-8/V cells, induce mitotic arrest at the G<sub>2</sub>/M phase with spindle abnormalities and promote apoptosis. Different from the published Plk1 inhibitors, Aristolactam AIIIa could bind to the interaction interface of CD/PBD due to targets both the catalytic domain and the polo-box domain of Plk1 kinase, and enhances the CD/PBD interaction. Our current work is expected to shed light on the potential antitumor mechanism of Aristolactam AIIIa, and this determined Plk1 inhibitor may also be used as a lead compound for further research.

## Abbreviations

Plk1: Polo-like kinase 1; CD: catalytic domain of Plk1; PBD: Polo box domain; HeLa: cell line taken from Henrietta Lacks alias Helen Lane; A549: human lung cancer A549 cell line; HGC:

human gastric cancer cell line; HCT-8/V: human colon adenocarcinoma cell line resistant to vincristine; SPR: Surface Plasmon Resonance; Plks: Polo-like kinases; Plk2: Polo-like kinase 2; SNK: serum inducible kinase; Plk3: Polo-like kinase 3; PRK: proliferation-related kinase; FNK: fibroblast growth factor-inducible kinase; Plk4: Polo-like kinase 4; SAK: Snk/Plk- $\alpha$ kin kinase; cdc2: cell division cycle 2 (cell cycle-dependent protein kinase); NudC: nuclear distribution gene C; NIH 3T3: mouse embryonic fibroblast cell line; ASONs: phosphorothioate antisense oligonucleotides; CDC25C: cell division cycle 25 homolog C; DMSO: dimethyl sulfoxide; HRP: horseradish peroxidase; 293T cell line: a derivative of human embryonic kidney cells line that stably express the large T-antigen of SV40; SRB: sulphorhodamine B; NVB: navelbine; PBS: phosphate-buffered saline; FITC: fluorescein isothiocyanate; PI: propidium iodide; PARP: poly [ADP-ribose] polymerase-1; ss-carrier DNA: salmon sperm-carrier DNA; SD medium: synthetic defined medium; 3-AT: 3-amino-10, 20, 40-triazole; IC<sub>50</sub>: concentration giving 50% of maximal inhibition; KB: human carcinoma cell (strain KB); P388: murine lymphoma cell (strain P388); HT29: a colon adenocarcinoma cell line (HT-29); HL60: human promyelocytic leukemia 60 cell line; L1210 cells: L1210 mouse leukemia cells; AA: arachidonic acid;  $K_D$ : dissociation constant; RUs: resonance units; MYT1: membrane-associated tyrosine- and threonine-specific cdc2-inhibitory kinase; CHK1: checkpoint kinase 1; CDK1: cyclin dependent kinase 1; PKC: protein kinase C.

## Acknowledgements

This work was supported by the State Key Program of Basic Research of China (grants 2010CB912501, 2009CB918502), the National Natural Science Foundation of China (grant 30890044), Shanghai Basic Research Project from the Shanghai Science and Technology Commission (grant 0811141013) and the Knowledge Innovation Program of the Chinese Academy of Sciences (grant SIMM0709QN-19).

## Author contribution

This study was designed by Xu WANG, Li LI, Jing CHEN, and Li-hong HU. The surface plasmon resonance (SPR) technology-based assay, enzymatic inhibition assay and cell-based assays which were used to screen and further identify Plk1 inhibitor were performed by Xu WANG, Li LI, Hong DING, and Jing CHEN. The experiments about investigating the potential inhibition mechanism of active compound against Plk1 were performed by Hong DING, Yu ZHANG, and Jing CHEN. Xu SHEN, Hua-liang JIANG, and Li-hong HU supervised the project. Li LI, Jing CHEN, Tian-cen HU, and Xu SHEN contributed to the manuscript writing. All authors read and approved the final manuscript.

## References

- 1 Glover DM, Hagan IM, Tavares AA. Polo-like kinases: a team that plays throughout mitosis. *Genes Dev* 1998; 12: 3777–87.
- 2 Hamanaka R, Maloid S, Smith MR, O'Connell CD, Longo DL, Ferris DK. Cloning and characterization of human and murine homologues of the *Drosophila* polo serine-threonine kinase. *Cell Growth Differ* 1994; 5: 249–57.
- 3 Simmons DL, Neel BG, Stevens R, Evett G, Erikson RL. Identification of an early-growth-response gene encoding a novel putative protein kinase. *Mol Cell Biol* 1992; 12: 4164–9.

- 4 Donohue PJ, Alberts GF, Guo Y, Winkles JA. Identification by targeted differential display of an immediate early gene encoding a putative serine/threonine kinase. *J Biol Chem* 1995; 270: 10351–7.
- 5 Ouyang B, Pan H, Lu L, Li J, Stambrook P, Li B, *et al*. Human Prk is a conserved protein serine/threonine kinase involved in regulating M phase functions. *J Biol Chem* 1997; 272: 28646–51.
- 6 Fode C, Motro B, Yousefi S, Heffernan M, Dennis JW. Sak, a murine protein-serine/threonine kinase that is related to the *Drosophila* polo kinase and involved in cell proliferation. *Proc Natl Acad Sci USA* 1994; 91: 6388–92.
- 7 Roshak AK, Capper EA, Imburgia C, Fornwald J, Scott G, Marshall LA. The human polo-like kinase, PLK, regulates cdc2/cyclin B through phosphorylation and activation of the cdc25C phosphatase. *Cell Signal* 2000; 12: 405–11.
- 8 Lane HA, Nigg EA. Antibody microinjection reveals an essential role for human polo-like kinase 1 (Plk1) in the functional maturation of mitotic centrosomes. *J Cell Biol* 1996; 135: 1701–13.
- 9 Sumara I, Vorlaufer E, Stukenberg PT, Kelm O, Redemann N, Nigg EA, *et al*. The dissociation of cohesin from chromosomes in prophase is regulated by Polo-like kinase. *Mol Cell* 2002; 9: 515–25.
- 10 Kotani S, Tugendreich S, Fujii M, Jorgensen PM, Watanabe N, Hoog C, *et al*. PKA and MPF-activated polo-like kinase regulate anaphase-promoting complex activity and mitosis progression. *Mol Cell* 1998; 1: 371–80.
- 11 Zhou T, Aumais JP, Liu X, Yu-Lee LY, Erikson RL. A role for Plk1 phosphorylation of NudC in cytokinesis. *Dev Cell* 2003; 5: 127–38.
- 12 Strebhardt K, Ullrich A. Targeting polo-like kinase 1 for cancer therapy. *Nat Rev Cancer* 2006; 6: 321–30.
- 13 Smith MR, Wilson ML, Hamanaka R, Chase D, Kung H, Longo DL, *et al*. Malignant transformation of mammalian cells initiated by constitutive expression of the polo-like kinase. *Biochem Biophys Res Commun* 1997; 234: 397–405.
- 14 Spänkuch-Schmitt B, Wolf G, Solbach C, Loibl S, Knecht R, Stegmüller M, *et al*. Downregulation of human polo-like kinase activity by antisense oligonucleotides induces growth inhibition in cancer cells. *Oncogene* 2002; 21: 3162–71.
- 15 Elez R, Piiper A, Kronenberger B, Kock M, Brendel M, Hermann E, *et al*. Tumor regression by combination antisense therapy against Plk1 and Bcl-2. *Oncogene* 2003; 22: 69–80.
- 16 Jang YJ, Lin CY, Ma S, Erikson RL. Functional studies on the role of the C-terminal domain of mammalian polo-like kinase. *Proc Natl Acad Sci USA* 2002; 99: 1984–9.
- 17 Elia AE, Rellos P, Haire LF, Chao JW, Ivins FJ, Hoepker K, *et al*. The molecular basis for phosphodependent substrate targeting and regulation of Plks by the Polo-box domain. *Cell* 2003; 115: 83–95.
- 18 Stevenson CS, Capper EA, Roshak AK, Marquez B, Eichman C, Jackson JR, *et al*. The identification and characterization of the marine natural product scytonemin as a novel antiproliferative pharmacophore. *J Pharmacol Exp Ther* 2002; 303: 858–66.
- 19 Stevenson CS, Capper EA, Roshak AK, Marquez B, Grace K, Gerwick WH, *et al*. Scytonemin – a marine natural product inhibitor of kinases key in hyperproliferative inflammatory diseases. *Inflamm Res* 2002; 51: 112–4.
- 20 Gumireddy K, Reddy MV, Cosenza SC, Boominathan R, Baker SJ, Papathi N, *et al*. ONO1910, a non-ATP-competitive small molecule inhibitor of Plk1, is a potent anticancer agent. *Cancer Cell* 2005; 7: 275–86.
- 21 Reindl W, Yuan J, Krämer A, Strebhardt K, Berg T. Inhibition of polo-like kinase 1 by blocking polo-box domain-dependent protein-protein interactions. *Chem Biol* 2008; 15: 459–66.
- 22 Priestap HA. Seven aristolactams from *Aristolochia* Argentina. *Phytochemistry* 1985; 24: 849–52.
- 23 Couture A, Deniau E, Grandclaudon P, Rybalko-Rosen H, Léonce S, Pfeiffer B, *et al*. Synthesis and biological evaluation of Aristolactams. *Bioorg Med Chem Lett* 2002; 12: 3557–9.
- 24 Kumar V, Poonam, Prasad AK, Parmar VS. Naturally occurring Aristolactams, aristolochic acids and dioxoaporphines and their biological activities. *Nat Prod Rep* 2003; 20: 565–83.
- 25 Skehan P, Storeng R, Scudiero D, Monks A, McMahon J, Vistica D, *et al*. New colorimetric cytotoxicity assay for anticancer-drug screening. *J Natl Cancer Inst* 1990; 82: 1107–12.
- 26 Diaz-Camino C, Risseuw EP, Liu E, Crosby WL. A high-throughput system for two-hybrid screening based on growth curve analysis in microtiter plates. *Anal Biochem* 2003; 316: 171–4.
- 27 Chia YC, Chang FR, Teng CM, Wu YC. Aristolactams and dioxoaporphines from *Fissistigma balansae* and *Fissistigma oldhamii*. *J Nat Prod* 2000; 63: 1160–3.
- 28 Cogswell JP, Brown CE, Bisi JE, Neill SD. Dominant-negative polo-like kinase 1 induces mitotic catastrophe independent of cdc25C function. *Cell Growth Differ* 2000; 11: 615–23.
- 29 Sumara I, Giménez-Abián JF, Gerlich D, Hirota T, Kraft C, de la Torre C, *et al*. Roles of polo-like kinase 1 in the assembly of functional mitotic spindles. *Curr Biol* 2004; 14: 1712–22.
- 30 Soldani C, Scovassi AI. Poly (ADP-ribose) polymerase-1 cleavage during apoptosis: an update. *Apoptosis* 2002; 7: 321–8.
- 31 Liu X, Erikson RL. Polo-like kinase (Plk) 1 depletion induces apoptosis in cancer cells. *Proc Natl Acad Sci USA* 2003; 100: 5789–94.
- 32 Steegmaier M, Hoffmann M, Baum A, Lénárt P, Petronczki M, Krssák M, *et al*. BI 2536, a potent and selective inhibitor of polo-like kinase 1, inhibits tumor growth *in vivo*. *Curr Biol* 2007; 17: 316–22.
- 33 Lee KS, Grenfell TZ, Yarm FR, Erikson RL. Mutation of the polo-box disrupts localization and mitotic functions of the mammalian polo kinase Plk. *Proc Natl Acad Sci USA* 1998; 95: 9301–6.